

High poloidal beta equilibria in the Tokamak Fusion Test Reactor limited by a natural inboard poloidal field null*

S. A. Sabbagh,[†] R. A. Gross, M. E. Mauel, and G. A. Navratil
Department of Applied Physics, Columbia University, New York, New York 10027

M. G. Bell, R. Bell, M. Bitter, N. L. Bretz, R. V. Budny, C. E. Bush, M. S. Chance, P. C. Efthimion, E. D. Fredrickson, R. Hatcher, R. J. Hawryluk, S. P. Hirshman,[‡] A. C. Janos, S. C. Jardin, D. L. Jassby, J. Manickam, D. C. McCune, K. M. McGuire, S. S. Medley, D. Mueller, Y. Nagayama, D. K. Owens, M. Okabayashi, H. K. Park, A. T. Ramsey, B. C. Stratton, E. J. Synakowski, G. Taylor, R. M. Wieland, and M. C. Zarnstorff

Plasma Physics Laboratory, Princeton University, Princeton, New Jersey 08543

J. Kesner, E. S. Marmor, and J. L. Terry

MIT Plasma Fusion Center, Massachusetts Institute of Technology, Cambridge, Massachusetts 02139

(Received 13 December 1990, accepted 1 April 1991)

Recent operation of the Tokamak Fusion Test Reactor (TFTR) [Plasma Phys. Controlled Nucl. Fusion Research **1**, 51 (1986)] has produced plasma equilibria with values of $\Lambda \equiv \beta_{p,eq} + I_p/2$ as large as 7, $\epsilon\beta_{p,dia} \equiv 2\mu_0 \epsilon \langle p_{\parallel} \rangle / \langle \langle B_p \rangle \rangle^2$ as large as 1.6, and Troyon normalized diamagnetic beta [Plasma Phys. Controlled Fusion **26**, 209 (1984); Phys. Lett. **110A**, 29 (1985)], $\beta_{N,dia} \equiv 10^8 \langle \beta_{t\parallel} \rangle a B_0 / I_p$ as large as 4.7. When $\epsilon\beta_{p,dia} \gtrsim 1.25$, a separatrix entered the vacuum chamber, producing a naturally diverted discharge that was sustained for many energy confinement times, τ_E . The largest values of $\epsilon\beta_p$ and plasma stored energy were obtained when the plasma current was ramped down prior to neutral beam injection. The measured peak ion and electron temperatures were as large as 24 and 8.5 keV, respectively. Plasma stored energy in excess of 2.5 MJ and τ_E greater than 130 msec were obtained. Confinement times of greater than 3 times that expected from L-mode predictions have been achieved. The fusion power gain Q_{DD} reached a value of 1.3×10^{-3} in a discharge with $I_p = 1$ MA and $\epsilon\beta_{p,dia} = 0.85$. A large, sustained negative loop voltage during the steady-state portion of the discharge indicates that a substantial noninductive component of I_p exists in these plasmas. Transport code analysis indicates that the bootstrap current constitutes up to 65% of I_p . Magnetohydrodynamic (MHD) ballooning stability analysis shows that, while these plasmas are near, or at the β_p limit, the pressure gradient in the plasma core is in the first region of stability to high- n modes.

I. INTRODUCTION

A significant concern regarding the next generation of tokamak fusion experiments and fusion reactor concepts is the large toroidal plasma current I_p needed to provide sufficient energy confinement to sustain fusion burn conditions in these devices. If improved confinement and adequate stability can be achieved, operation at high poloidal beta β_p can alleviate many problems associated with conventional tokamak reactor designs.^{1,2} Operation at lower I_p associated with high β_p considerably reduces the adverse consequences of plasma disruptions. The power requirements for steady-state current drive are reduced at lower I_p . In addition, a significant amount of neoclassical bootstrap current³⁻⁵ is predicted to form at high β_p , which could further reduce current drive requirements.

Capitalizing on these advantages, several reactor design studies including the ARIES⁶ and the JAERI Steady-State

Tokamak Reactor, SSTR⁷ designs, have incorporated fusion plasma operation at high β_p . However, since experience from the operation of large tokamaks has generally been at relatively small values of β_p (less than the tokamak aspect ratio), high- β_p reactor designs have been considered speculative, regardless of the benefits they may present. The demonstration of stable, high- β_p plasma operation in present large tokamak devices would begin to provide the experimental basis for the design of such a high- β_p reactor.

This paper presents results from recent experiments in the Tokamak Fusion Test Reactor, TFTR,⁸ which have produced plasmas with very large values of β_p . While high- β_p plasmas have been achieved in other tokamaks,⁹⁻¹² these are the first experiments that demonstrate stable plasma equilibria, limited by a natural inboard poloidal field null at high β_p , that are sustained for many energy confinement times τ_E in a large neutral beam heated device. The methods employed to produce these plasmas and the plasma parameters achieved are described in the next section. A preliminary analysis of stability, confinement, noninductive current drive, and neutron production for these high- β_p plasmas is presented in the subsequent sections.

*Paper 4I6, Bull. Am. Phys. Soc. **35**, 1992 (1990).

[†] Invited speaker. Present address: Princeton Plasma Physics Laboratory, Princeton University, Princeton, NJ 08543.

[‡] Present address: Oak Ridge National Laboratory, Oak Ridge, Tennessee 37830.

II. PLASMA PARAMETERS AND OPERATION AT HIGH β_p

Stable plasmas with $\beta_{p \text{ dia}} \leq 5.9$ and $\epsilon\beta_{p \text{ dia}} \leq 1.6$ were created in TFTR, surpassing an apparent limiting value of $\epsilon\beta_{p \text{ dia}} \leq 0.7$ previously observed in TFTR supershots.^{13,14} Here, $\beta_{p \text{ dia}} \equiv 2\mu_0 \langle p_\perp \rangle / \langle \langle B_p \rangle \rangle^2$, where $\langle p_\perp \rangle$ is the volume average of the transverse plasma pressure and $\langle \langle B_p \rangle \rangle$ is the line average of the poloidal magnetic field taken over the outer flux surface. The inverse-aspect-ratio is $\epsilon \equiv a/R_p$, with the minor radius a defined as one-half of the midplane width and R_p defined as the area-averaged major radius. The Troyon¹⁵ normalized diamagnetic beta, $\beta_{N \text{ dia}} \equiv 10^8 \langle \beta_{ti} \rangle \times a B_0 / I_p$, reached 4.7. For comparison, TFTR supershots had previously reached values of $\beta_{N \text{ dia}} \leq 2.7$.¹⁶ Here, B_0 is the vacuum toroidal field at R_p . Figure 1, which shows $\epsilon\beta_{p \text{ dia}}$ as a function of $q^* \equiv 5(a^2 B_0 / R_p I_p)(1 + \kappa^2)/2$, illustrates how the high- β_p plasmas extend the range of supershot operation in TFTR. Here, κ is the plasma elongation. As $\epsilon\beta_{p \text{ dia}}$ is increased to a value of approximately 1.25, the plasma that is initially limited on the inside wall makes a transition to a diverted plasma, the boundary being defined by a naturally occurring separatrix with a poloidal field null on the inboard side. At the larger values of q^* , the value of $\epsilon\beta_{p \text{ dia}}$ is limited by the separatrix moving further into the plasma minor radius. At the smaller values of q^* , the plasmas encounter a beta limit, but with a value of β_N much larger than the limit of 3.0 originally proposed by Troyon.¹⁵

These plasmas were created in deuterium at relatively small I_p (0.28–1.0 MA during neutral beam heating), nominal $B_0 = 4.8$ T, and $R_p = 2.45$ m. Separatrix-limited discharges were created with two types of I_p time histories, one in which I_p was held constant and another in which I_p was decreased, or ramped down, before the start of neutral beam injection. In the latter case, an Ohmic plasma was formed with I_p in the range of 0.85–1.75 MA and held for about 1 sec. The plasma current was then decreased rapidly at -2.5 MA/sec to a pedestal value in the range of 0.3–1.0 MA. The maximum ratio of initial to pedestal I_p was about 2.5. In some discharges, beam injection was started before I_p had

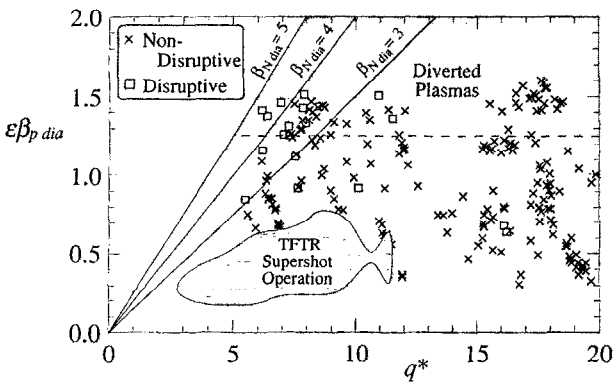


FIG. 1. $\epsilon\beta_{p \text{ dia}}$ for high- β_p discharges in TFTR plotted as a function of q^* . The high- β_p discharges have extended TFTR operation to larger values of q^* , $\epsilon\beta_{p \text{ dia}} \leq 1.6$, and $\beta_{N \text{ dia}} \leq 4.7$. Contours of $\beta_{N \text{ dia}}$ appear as straight lines in this figure.

been fully decreased to the pedestal value. The largest values of $\epsilon\beta_{p \text{ dia}}$ and $\beta_{N \text{ dia}}$ were obtained in discharges in which I_p was ramped down. Neutral beam heating, utilizing tangential injection of deuterium, usually began with coinjection only. Subsequently, counter-injected beams were added to provide nearly balanced co- and counter injection at 18–26 MW during the high- $\epsilon\beta_p$ steady state. Line-averaged target densities were in the range of $(1-3) \times 10^{19} \text{ m}^{-3}$ and typically increased to $(3-6) \times 10^{19} \text{ m}^{-3}$ during the auxiliary heating phase.

Waveforms illustrating the I_p ramp-down and separatrix formation are shown in Fig. 2. An Ohmic plasma was initially formed with $I_p = 0.85$ MA [Fig. 2(a)]. The plasma current was ramped down and held approximately constant at 0.4 MA during the neutral beam heating phase. In this particular discharge, I_p decreased at a small rate (-0.05 MA/sec) after the fast I_p ramp down had been completed. This was caused by the finite ability of the plasma control system to hold I_p at an exactly programmed value while other plasma quantities, particularly β_p , were changing rapidly. The voltage associated with this slow decrease in I_p is approximately -0.25 V, which is a small fraction of the -1.5 V surface voltage measured during the high- β_p phase of the discharge.

Figure 2(b) shows the evolution of $\beta_{p \text{ dia}}$ and $\Lambda \equiv \beta_{p \text{ eq}} + l_i/2$, with l_i being the plasma internal inductance. At maximum stored energy, this discharge attained values of $\epsilon\beta_{p \text{ dia}} = 1.43$ and $\beta_{N \text{ dia}} = 3.4$ with $q^* = 8.5$. As a result of the tangential beam injection, these discharges are anisotropic and $\beta_{p \text{ eq}} \equiv (\beta_{p \parallel} + \beta_{p \perp})/2$ is larger than

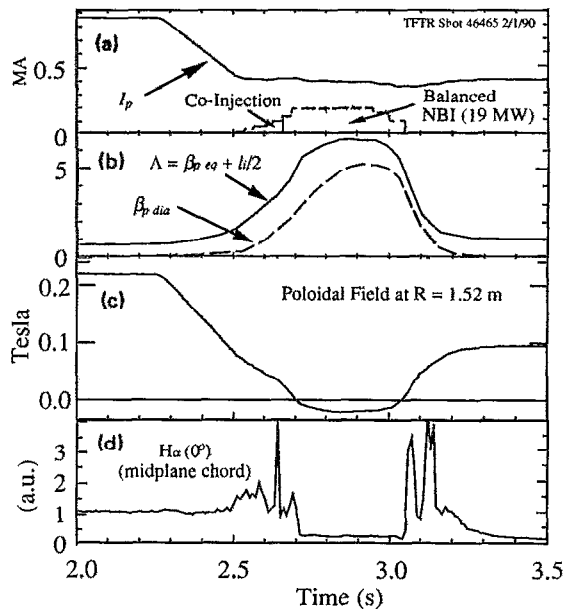


FIG. 2. Time history waveforms for a high- β_p discharge with I_p ramp-down. Shown are (a) the plasma current and neutral beam heating, (b) Λ and $\beta_{p \text{ dia}}$, (c) the poloidal field at the midplane, on the inboard side of the vacuum vessel, and (d) the midplane H_α emission. As $\beta_{p \text{ dia}}$ rises, a separatrix enters the vacuum vessel, as indicated by the reversal of the midplane poloidal field measured just outside the inboard side of the vacuum vessel, and by a sharp drop in the midplane H_α emission.

$\beta_{p \text{ dia}} \equiv \beta_{p1}$. The calculated ratio of $\beta_{p\parallel}/\beta_{p1}$ varies throughout the beam heating phase. Modeling of the discharge shown in Fig. 2 using the TRANSP code¹⁷ indicates that the ratio $\beta_{p\parallel}/\beta_{p1}$ reaches a maximum value of 1.65 that occurs 100 msec after the start of beam injection. This ratio decreases to 1.15 by the end of the beam injection.

Figure 2(c) shows the evolution of the poloidal field measured at the midplane on the inboard side of the TFTR vacuum vessel. As I_p is ramped down, and β_p increases, the midplane poloidal field decreases and eventually becomes negative, indicating that the separatrix has crossed the coil position and moved into the vacuum vessel. The separatrix-limited discharge is sustained until the end of the beam heating phase. Figure 2(d) shows the H_α emission, viewed along the plasma midplane (0°). As the separatrix enters the vacuum vessel, and the divertor X point moves into the plasma, the H_α emission at 0° drops to a low level and remains low throughout the separatrix-limited phase.

Additional details of the H_α emission signatures characteristic of the separatrix-limited plasmas in TFTR are shown in Fig. 3. Here, the evolution of the plasma boundary from the discharge shown in Fig. 2 is reconstructed from a magnetic analysis code that uses external magnetic measurements and models the plasma current distribution as a collection of current filaments.^{18,19} Included in the figure are the H_α emission time histories from four chords viewing different poloidal angles as shown. While the H_α emission shows some fluctuation, no large-scale magnetohydrodynamic (MHD) modes or significant loss of plasma stored energy is observed to correlate with this activity. At 2.5 sec, the plasma is essentially circular and limited on the inner belt limiter. At 2.7 sec, the separatrix is entering the vacuum vessel, the plasma becomes more oblate, and $H_\alpha(0^\circ)$ drops. There is a similar drop in the H_α emission at 7.5° somewhat later in time as the X point moves further into the vessel and the divertor strike points move to greater poloidal angles. This progression of the strike points eventually ceases as the

equilibrium is reached at approximately 2.9 sec, and, subsequently, $H_\alpha(14^\circ)$ remains at a large value. The chord at 23° being outside of the range of the strike point, exhibits a more standard emission trace. This evolution of the inboard X point has also been observed using a visible-light camera that tangentially views the inside of the TFTR vacuum vessel.

A subset of the separatrix-limited equilibria has been modeled using a free-boundary equilibrium code²⁰ based on the technique of Lao and co-workers²¹ that uses external magnetic measurements plus measurements of the local internal poloidal field from polarimetry of emission from injected Li pellets.²² Data from 14 similar discharges were used to calculate the mean and standard deviation of the measurements. Note that the equilibrium reconstruction assumes that the measured errors are statistically independent and that the pressure is isotropic. Figure 4 shows the reconstructed poloidal field profile fitted to the measured internal poloidal field data and the poloidal flux contours for the least squares "best fit" equilibrium. This technique provides a measurement of the q profile. For the 0.3 MA constant I_p discharge shown in Fig. 4, $\Lambda = 5.1 \pm 0.3$, $\beta_{p \text{ eq}} = 1.38 \pm 0.12$ and $q_0 = 1.6 \pm 0.55$. This is in good agreement with $\Lambda = 5.3 \pm 0.5$ obtained from filament code modeling. The large calculated Shafranov shift of the magnetic axis agrees with the axis position inferred from soft x-ray measurements. Measurements of the electron temperature T_e , density n_e , and ion temperature T_i also exhibit this large outward axis shift. Peak $T_i = 24$ keV and $T_e = 8.5$ keV (T_e measured by Thomson scattering) have been achieved in these high- β_p TFTR plasmas.

III. STABILITY AND β LIMIT

Values of $\epsilon\beta_{p \text{ dia}} > 1.5$ have been reached in discharges in which I_p was ramped down as well as in plasmas in which I_p

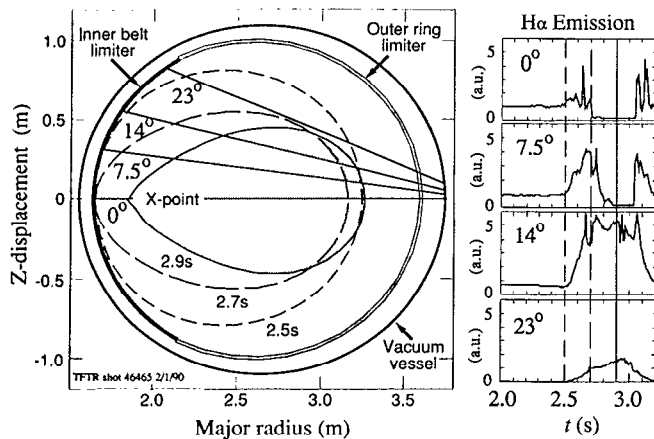


FIG. 3. Evolution of the plasma outer boundary and H_α emission for the high- β_p discharge of Fig. 2. The plasma makes a transition from a circular discharge limited on the inner belt limiter, to an oblate separatrix-limited discharge. A drop in the H_α emission is observed at 0° and 7.5° as the separatrix enters the vessel and the divertor strike points move to greater poloidal angles.

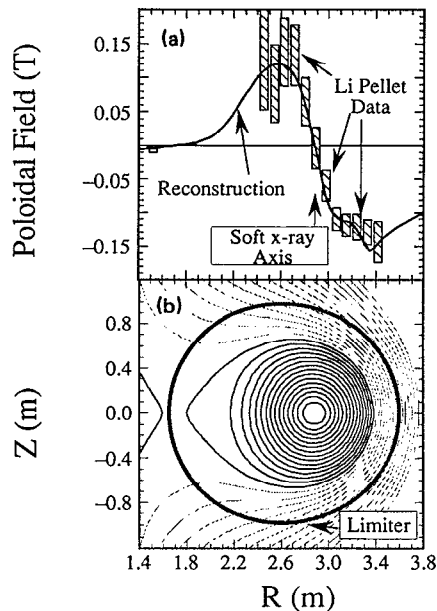


FIG. 4. Free-boundary equilibrium reconstruction of a 0.3 MA, constant I_p discharge. (a) The internal poloidal magnetic field measurements and the least squares "best fit" poloidal field profile reconstruction. (b) The poloidal flux contours for the equilibrium.

was held constant. At values of $q^* \gtrsim 10$ ($\beta_{N \text{ dia}} \lesssim 2.7$), the maximum value of $\epsilon\beta_{p \text{ dia}} \sim 1.6$ attained in these plasmas appears to be due to a limit imposed by the approach of the separatrix. At these large values of q^* , the maximum value of $\beta_{N \text{ dia}}$ attained is due to the constraint on $\epsilon\beta_{p \text{ dia}}$ and is not associated with disruption or a soft decay in β due to plasma instability.

The maximum value of $\beta_{N \text{ dia}}$ reached in the high- β_p TFTR discharges exceeds that of previous TFTR supershot discharges by a factor of about 1.75. The largest values of $\beta_{N \text{ dia}}$ were obtained in discharges in which I_p was ramped down. This is illustrated in Fig. 5, where for a subset of the high- β_p database, $\beta_{N \text{ dia}}$ is plotted as a function of the plasma current ramp ratio F_{I_p} , defined as the ratio of I_p before the ramp down, to I_p during the neutral beam heating phase. For example, the discharge illustrated in Fig. 2 has $F_{I_p} = 2.2$. The subset excludes some constant I_p discharges for clarity. No disruptions or large-scale MHD activity were observed for high β_p , constant I_p plasmas that had $1 \leq \beta_{N \text{ dia}} \leq 2.3$. Relatively few disruptions were encountered for all plasmas with $\beta_{N \text{ dia}} \leq 3.6$. Above this value, the fraction of discharges ending in disruption increased dramatically. Many of these discharges disrupted after β had reached saturation, indicating that profile relaxation toward an unstable state may have been the cause of disruption. The disruptions at high β_N were fast (on an ideal MHD time scale), and showed no clear precursors. Soft β collapse was also observed in high- β_N discharges with $q^* \lesssim 10$. Analysis of the Mirnov signal phase shows that the dominant mode is $m/n = 2/1$, where m and n are the poloidal and toroidal mode numbers, respectively. The $m/n = 3/2$ mode usually accompanies this mode, but at a lower amplitude. The onset of MHD activity leading to a β collapse frequently occurred in discharges that had a larger fraction of coinjected beam power than counter-injected. Sawtooth activity was generally absent from the high- β_p discharges except those with the largest values of I_p (0.85–1.0 MA).

At larger values of $I_p \gtrsim 0.8$ MA, and at moderate values of $\epsilon\beta_{p \text{ dia}} \lesssim 1$, the discharges have been observed to make a transition into the limiter H mode.²³ This transition occurs more easily in discharges in which I_p is ramped down.²⁴ The limiter H mode in TFTR is accompanied by edge-localized

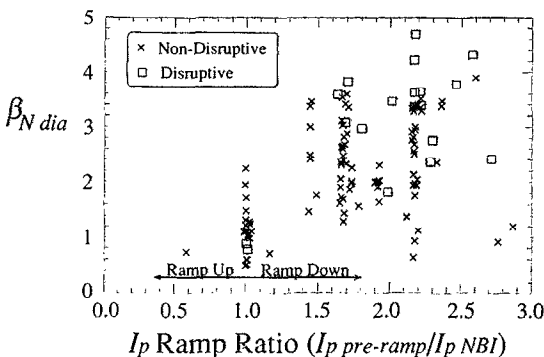


FIG. 5. Troyon-normalized diamagnetic β as a function of plasma current ramp ratio. The maximum value of $\beta_{N \text{ dia}}$ increases as the plasma current ramp ratio increases.

modes (ELM's) which appear to cause β saturation or degradation. A transition to the limiter H mode generally does not occur at large $q^* \gtrsim 10$ and large $\epsilon\beta_{p \text{ dia}} \gtrsim 1$.

The enhanced plasma stability, indicated by the achievement of increased values of $\beta_{N \text{ dia}}$ when I_p is ramped down, appears to be associated with the peaking of the plasma current profile, as shown by the increased value of l_i , during the high- β_p phase of the discharges. Figure 6 shows the maximum value of $\beta_{N \text{ dia}}$ as a function of $l_i/2$ for a subset of the high- β_p equilibria analyzed by the TRANSP code; data for some supershot discharges are also shown. Here, $l_i \equiv \langle B_p^2/2\mu_0 \rangle / \langle B_p^2/2\mu_0 \rangle_{\text{dva}}$, where $\langle B_p^2 \rangle_{\text{dva}}$ is the differential volume average of B_p^2 over the outermost flux surface. Cases in which I_p was ramped up have smaller values of l_i while those in which I_p was ramped down have larger values of l_i . The plasma current profile peakedness changes in response to the programmed plasma current and high- β_p equilibrium effects for each discharge. During I_p ramp-down, the surface voltage reverses in order to decrease the plasma current. TRANSP code analysis of the current profile evolution shows a reduction, or in some cases, a reversal of the plasma current in the outer 1/3 of the plasma. The I_p ramp-down causes the edge q to rise and l_i to increase. A further increase in l_i occurs as the high- β_p state is reached. Later in the high- β_p phase, l_i generally decreases as the plasma current is resistively redistributed and as the bootstrap current fraction increases.

In addition, Fig. 6 shows the trajectory of two different discharges, one that encounters disruption, and another that does not. In both cases, neutral beam heating commences when $\beta_{N \text{ dia}}$ begins to increase. The point of completion of the I_p ramp-down in each discharge is indicated in the figure. For the trajectory marked by label (a) in Fig. 6, I_p was ramped down from 0.85 to 0.4 MA. The $\beta_{N \text{ dia}}$ increases throughout the discharge, whereas l_i first increases and subsequently decreases as described above, leading to disrupt-

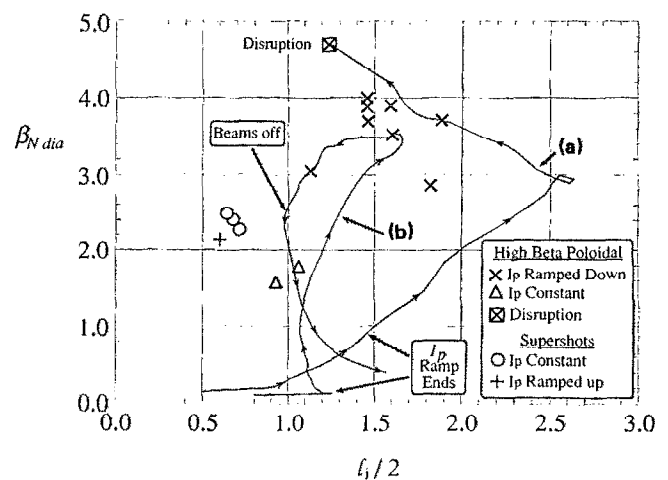


FIG. 6. Troyon-normalized diamagnetic β as a function of plasma internal inductance. The points represent the maximum $\beta_{N \text{ dia}}$ attained for each discharge. Trajectory (a) pertains to a discharge in which I_p was ramped down from 0.85 to 0.4 MA. Trajectory (b) pertains to a discharge in which I_p was ramped down from 1.0 to 0.7 MA. The maximum value of $\beta_{N \text{ dia}}$ increases for discharges in which l_i is increased.

tion. For trajectory (b), I_p was ramped down from 1.0 to 0.7 MA. The $\beta_{N\text{dia}}$ initially increases as I_i increases, but $\beta_{N\text{dia}}$ subsequently decreases coincident with a decrease in I_i . This plasma does not terminate in disruption but rather a soft β decay leads to the reduction in $\beta_{N\text{dia}}$. Neutral beam heating terminates as $\beta_{N\text{dia}}$ and I_i are decreasing. In other high- β_p cases, $\beta_{N\text{dia}}$ saturates and remains large until the end of the beam pulse.

The observation of increased $\beta_{N\text{dia}}$ associated with an increase in I_i is similar to results of experiments performed on the DIII-D tokamak.²⁵ This observation does not appear to be machine dependent, since the TFTR experiments were performed in a circular vacuum vessel with oblate plasmas ($\kappa \sim 0.7$) and I_n in the range $0.08 < I_n < 0.3$, where $I_n \equiv I/aB_0$ (MA/m/T), compared with elongated plasmas ($\kappa < 1.9$) and $1.0 < I_n < 1.4$ in DIII-D.

High- n ballooning analysis of these discharges was performed on both the free-boundary equilibria reconstructed from external and internal magnetic field data described earlier and equilibria generated using profile and outer-boundary information from the TRANSP code. The results show that these plasmas are in the first region of stability to high- n modes. Figure 7 shows the stability results for an equilibrium constructed from TRANSP-calculated profiles for a plasma in which I_p was ramped down from 0.85 to 0.4 MA. The q_0 is calculated to be 1.1 for this particular equilibrium. The plasma pressure gradient $p'(\psi)$ is plotted as a function of a minor radial flux coordinate $\sqrt{(\psi - \psi_0)/(\psi_a - \psi_0)}$ (subscripts "a" and "0" correspond to the values at the plasma edge and magnetic axis, respectively), where ψ is the poloidal flux. Pressure gradients that lie inside the shaded region are unstable. Those that lie below are stable in the first stability region, while those that lie above are in the second stability region. The equilibrium $p'(\psi)$ is in the first stable region in the plasma core, and lies on the first-region boundary in the outer portion of the plasma. The stability of these plasmas on the outermost flux surfaces is uncertain, since the error associated with the $p'(\psi)$ profile is of the order of the width of the unstable region at the plasma edge. Note that the beam particle pressure gradient is included in the scalar pressure used for these equilibrium and stability calculations.

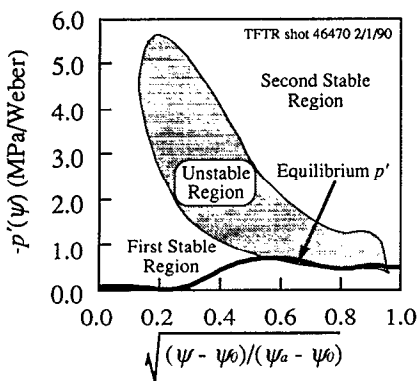


FIG. 7. High- n ballooning stability for a high- β_p discharge in which I_p is ramped down. The plasma pressure gradient is in the first region of high- n ballooning stability.

tions. The beam component of the pressure constitutes 58% of the total pressure on axis in the equilibrium in Fig. 7.

IV. ENERGY CONFINEMENT

Energy confinement times of greater than 3 times L-mode values have been obtained in these high- β_p plasmas, similar to the enhancement reached in supershot plasmas. Figure 8 shows τ_E normalized to that computed from the ITER 89-P energy confinement scaling relation²⁶ as a function of $\epsilon\beta_{p\text{dia}}$ for a subset of the high- β_p database. There is a general increase in the confinement enhancement as $\epsilon\beta_{p\text{dia}}$ increases, and plasmas in which I_p is ramped down have the largest enhancement factors. Note that the confinement time data was taken at the time of maximum transverse stored energy, and $\tau_E \equiv E_{\text{tot}}/P_{\text{beam}}$, where E_{tot} is the plasma-stored energy and P_{beam} is the beam power. The Ohmic power P_{Ohmic} is small for these cases. The ratio $P_{\text{Ohmic}}/P_{\text{beam}} < 0.06$ at the largest I_p and is usually much smaller at lower I_p . Absolute values of τ_E reach 130 msec in these plasmas. Values of E_{tot} of about 2.5 MJ have been attained in plasmas with $I_p = 0.83$ MA. The high- β_p plasmas generally show an improvement in the absolute value of τ_E as I_p is increased.

A significant improvement in τ_E is observed in plasmas in which I_p was ramped down to a specified value, compared to equivalent discharges in which I_p was held constant. For example, the discharge shown in Fig. 2, where I_p was decreased from 0.85 to 0.4 MA before neutral beam injection at $P_{\text{beam}} = 19$ MW, had $\tau_E = 45$ msec. A discharge with the same heating power and constant $I_p = 0.4$ MA had $\tau_E = 28$ msec. By starting beam injection 100 msec before I_p had been fully ramped down from 0.85 to 0.4 MA, $\tau_E = 64 \pm 5$ msec was attained at $P_{\text{beam}} = 17$ MW, more than doubling the value obtained at constant I_p . A similar relative increase in τ_E has been observed in other experiments on TFTR²⁷ and ASDEX²⁸ in which I_p was varied during the neutral beam injection phase of the discharge.

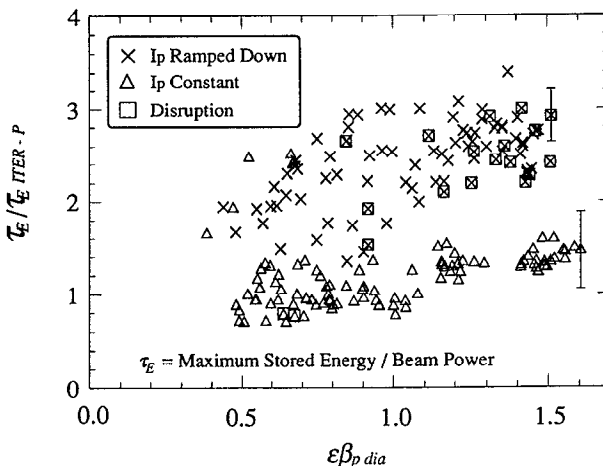


FIG. 8. Energy confinement enhancement as a function of $\epsilon\beta_{p\text{dia}}$ for high- β_p discharges. The largest enhancement factors occur in plasmas in which I_p was ramped down. The representative error bars shown arise from the uncertainty in the stored energy as calculated from magnetics measurements.

V. NONINDUCTIVE CURRENTS AND CURRENT PROFILE CONTROL

The high- β_p plasmas in TFTR have low collisionality for both ions and electrons. Under these conditions, a significant amount of bootstrap current should contribute to I_p . Shown in Fig. 9 is the time evolution of I_p , surface voltage, and $\beta_{p \text{ dia}}$ for a discharge in which I_p was ramped down from 1.0 to 0.6 MA. The parameters ν_e^* and ν_i^* for this discharge at 3.9 sec are 0.1 and 0.02 at one-half of the minor radius. Included with the time history waveforms are the noninductive current components of I_p and the surface voltage calculated by TRANSP. As the current is decreased before the beam injection, the surface voltage swings negative, removing 0.29 Wb of poloidal flux from the plasma between 3.0 and 3.25 sec. The plasma current profile is primarily affected in the outer 1/3 of the plasma, and the classical time constant associated with this change is about 0.3 sec. Since the coinjector beams are switched on first, there is initially a large fraction of codirected current driven by the beams. In this discharge, there is 37% more counter-injected power than coinjector power during the high- β_p phase. Since the coinjector beamlines drive current more efficiently than the counter beamlines because of orbit effects, this produces no net beam driven current. The bootstrap current is calculated to be 65% of the total I_p in this case. Similar results were obtained for discharges with balanced neutral beam injection. In these calculations, any potential contribution to the bootstrap current due to the anisotropic beam-particle pressure gradient has been neglected. The beam-particle pressure constitutes approximately 45% of the total plasma pressure in the plasma core at the end of the discharge.

In both constant current, and I_p ramp-down cases, there is a significant reversal of the surface voltage during the high- β_p portion of the discharge, as shown in Fig. 9. The

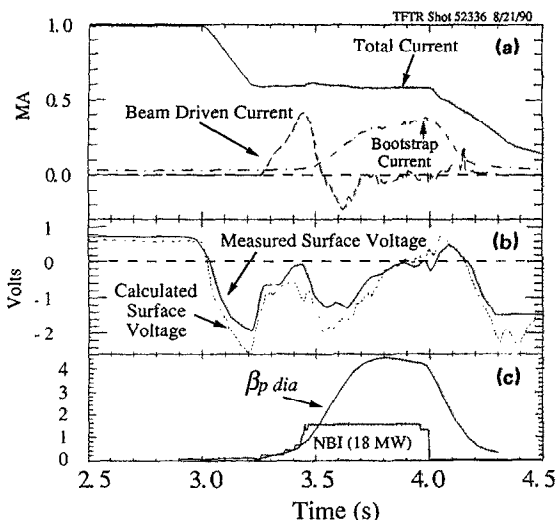


FIG. 9. Calculated noninductive current contributions to I_p . (a) I_p and the calculated noninductive beam- and bootstrap-driven components of I_p , (b) the measured and calculated plasma surface voltage, and (c) the evolution of $\beta_{p \text{ dia}}$ and neutral beam heating. The bootstrap current constitutes up to 65% of I_p for this discharge. The calculated surface voltage waveform is in good agreement with the measured waveform.

largest bootstrap current fractions were calculated to occur in I_p ramp-down cases. The surface voltage remains negative for the duration of the beam pulse, relaxing from less than -1 to about -0.2 V. A total of 0.35 Wb of poloidal flux was measured to be removed from the plasma between 3.4 and 4.0 sec. The classical time constant associated with this change is about 1 sec.

VI. NEUTRON PRODUCTION AND FUSION POWER GAIN

Neutron production in the high- β_p discharges at the larger values of I_p (0.85–1.0 MA) is comparable to TFTR supershot performance. Shown in Fig. 10 is the maximum neutron rate S_n plotted as a function of maximum beam power $P_{\text{beam max}}$ for discharges with $I_p \geq 0.5$ MA and $\epsilon\beta_{p \text{ dia}} \geq 0.7$. Also shown is the nominal supershot neutron production performance as a function of beam power.²⁹ Discharges that have S_n within 20% of this curve have $0.75 < \epsilon\beta_{p \text{ dia}} < 1.12$. At a plasma current of about 0.85 MA, neutron rates of $(1.5\text{--}1.9) \times 10^{16} \text{ sec}^{-1}$ have been achieved during the discharge and were sustained for 0.3–0.4 sec until neutral beam heating was terminated. For example, $S_n = 1.7 \times 10^{16} \text{ sec}^{-1}$ was reached at $I_p = 0.82$ MA, $E_{\text{tot}} = 2.3$ MJ, $\epsilon\beta_{p \text{ dia}} = 0.89$, and $P_{\text{beam max}} = 19$ MW. The corresponding deuterium–deuterium fusion power gain Q_{DD} is 1.1×10^{-3} . At $I_p = 0.97$ MA, $S_n = 2.63 \times 10^{16} \text{ sec}^{-1}$ was reached transiently with $E_{\text{tot}} = 2.8$ MJ, $\epsilon\beta_{p \text{ dia}} = 0.85$, and $P_{\text{beam max}} = 24$ MW, yielding $Q_{\text{DD}} = 1.3 \times 10^{-3}$. This Q_{DD} is 70% of the best value achieved in TFTR, obtained in a discharge that had $I_p = 1.9$ MA.

At a fixed plasma current, there is a large increase in the neutron production but only a small gain in Q_{DD} in high- β_p discharges as compared to supershots where the domains of these discharges overlap. At $I_p = 0.8$ MA and $P_{\text{beam max}} = 14$ MW, supershot discharges yield $S_n = 1.0 \times 10^{16} \text{ sec}^{-1}$. At $I_p = 1.0$ MA and $P_{\text{beam max}} = 18$ MW, $S_n = 1.6 \times 10^{16} \text{ sec}^{-1}$ has been reached. The high- β_p discharge mentioned above produced more neutrons than

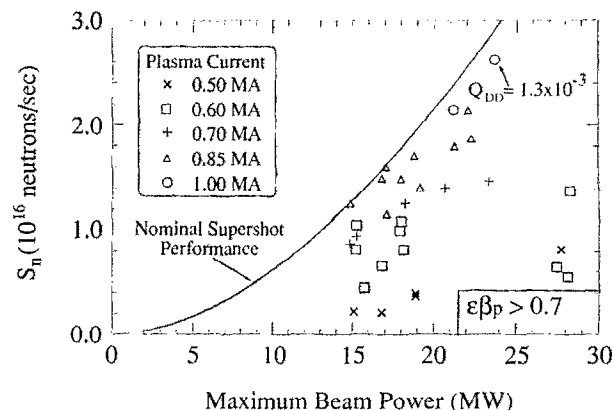


FIG. 10. Maximum neutron rate as a function of maximum beam power for discharges with $I_p \geq 0.5$ MA and $\epsilon\beta_{p \text{ dia}} \geq 0.7$. The curve describing the nominal neutron rate for TFTR supershots is superimposed for reference. Neutron production in high- β_p discharges with $I_p \geq 0.85$ MA is comparable to supershot discharges.

that achieved in the $I_p = 1$ MA supershot by greater than a factor of 1.6. This increase in the neutron rate comes about from the larger beam power that can be tolerated at a given I_p in the high- β_p discharges before a plasma disruption occurs. To obtain S_n equal to that of the high- β_p discharge with $I_p = 1$ MA, the plasma current in the supershot case needs to be raised to about 1.35 MA. The neutral beam heating power for this supershot case with equivalent S_n would be 22 MW, slightly less than was used in the $I_p = 1$ MA high- β_p case. Note that Q_{DD} is 1.2×10^{-3} in the $I_p = 1$ MA supershot discharge, which is essentially equal to the value reached in the high β_p discharge at the same plasma current but at larger beam power.

VII. SUMMARY AND DISCUSSION

The operating range of TFTR plasmas has been expanded to include plasmas with $\epsilon\beta_{p\text{ dia}}$ up to 1.6 and $\beta_{N\text{ dia}}$ up to 4.7. The range of I_p during neutral beam injection was 0.28 MA $< I_p < 1.0$ MA. At $\epsilon\beta_{p\text{ dia}}$ above 1.25, a natural inboard poloidal field null is observed to enter the vacuum vessel. The high- β_p separatrix forms a stable, diverted plasma with an oblate shape ($\kappa \sim 0.7$). The maximum value of $\epsilon\beta_{p\text{ dia}}$ for $q^* > 8$ is apparently due to an equilibrium limit as the X point moves further into the plasma minor radius. The largest values of $\epsilon\beta_{p\text{ dia}}$ and $\beta_{N\text{ dia}}$ are obtained when I_p is ramped down. Stable operation at large $\beta_{N\text{ dia}}$ is associated with increased plasma internal inductance, or peaked current profile. The only active current profile control in these discharges is provided by the Ohmic heating transformer, acting as a source of anticurrent drive during the I_p ramp-down and high- β_p phases of the discharges. Noninductive currents also reshape the current profile, with the bootstrap current calculated to comprise a significant component. The bootstrap current is calculated to constitute as much as 65% of the total current in these plasmas. The energy confinement properties of these discharges are significantly enhanced over L mode prediction. Energy confinement times greater than three times those expected from the ITER-89P scaling relation have been reached. This enhancement factor appears to increase as $\epsilon\beta_{p\text{ dia}}$ increases up to the equilibrium limit. Absolute values of τ_E and E_{tot} have reached 130 msec and 2.8 MJ, respectively. At a given neutral beam power, discharges in which I_p was ramped down to a specified value had substantially larger τ_E than in discharges in which I_p was held constant. The neutron production of the high- β_p plasmas with the largest I_p is comparable to that of standard supershot performance at a given neutral beam power level, but at significantly reduced plasma current. The Q_{DD} has reached 1.3×10^{-3} in a plasma with $I_p = 1$ MA and $\epsilon\beta_{p\text{ dia}} = 0.85$.

This demonstration of successful plasma operation near the equilibrium limit, and at large values of $\beta_{N\text{ dia}}$ with proper plasma current profile control, supports high-performance fusion reactor designs, such as ARIES and the JAERI SSTR, and future tokamak experiments operating at reduced I_p . The present experiments also point out several important considerations for future high- β tokamak designs. The first is inclusion of current drive to provide not only steady-state operation, but also current profile shape control. In the present experiments, the Ohmic heating

transformer only provides control of the plasma current density in the outer portion of the plasma. A technique such as lower-hybrid current drive, which can drive current efficiently near the plasma edge may therefore be sufficient to provide and sustain a current profile shape leading to a stable plasma exhibiting enhanced β_N performance. Since this system would be operating in a plasma with reduced I_p and only in a region of relatively small current density, the power requirements could be kept low. Another key consideration is the role of the bootstrap current, which will drive codirected plasma current, and hence may reduce the externally driven current required for steady-state operation. However, the bootstrap effect will broaden the current profile and reduce I_i which, in the present experiments, is associated with a reduction of the β_N at which the tokamak can operate in a stable fashion. The competing nature of these two effects needs to be carefully considered in high- β tokamak designs that would operate in the first stability region. A more detailed physics analysis of the improved stability and confinement of these high- β_p discharges is presently underway.

ACKNOWLEDGMENTS

The authors would like to thank M. W. Phillips of Grumman Corporation for making available the EQGRUM and STBAL equilibrium and stability codes used in the present analysis. We also thank Rob Goldston and Dale Meade for their encouragement, and the entire staff of the TFTR project for providing a reliable and well-diagnosed machine for these experiments.

This work was supported by US Department of Energy Contracts No. DE-FG02-89ER53297, No. DE-AC02-76-CHO-3073, and No. DE-FG02-90ER54084.

¹ K. Tomabeche and the ITER group, in *Plasma Physics and Controlled Nuclear Fusion Research*, Proceedings of the 12th International Conference, Nice, 1988 (IAEA, Vienna 1989), Vol. 3, p. 215.

² J. Sheffield, *J. Fusion Energy* **4**, 187 (1985).

³ M. C. Zarnstorff, M. G. Bell, M. Bitter, R. J. Goldston, B. Grek, R. J. Hawryluk, K. Hill, D. Johnson, D. McCune, H. Park, A. Ramsey, G. Taylor, and R. Wieland, *Phys. Rev. Lett.* **60**, 1306 (1988).

⁴ A. A. Galeev, *Zh. Eksp. Teor. Fiz.* **59**, 1378 (1970) [*Sov. Phys. JETP* **32**, 752 (1971)].

⁵ R. J. Bickerton, J. W. Connor, and J. B. Taylor, *Nature (London) Phys. Sci.* **229**, 110 (1971).

⁶ T. K. Mau, E. Ibrahim, G. Emmert, J. F. Santarius, and the ARIES design team, *Bull. Am. Phys. Soc.* **35**, 2131 (1990).

⁷ M. Kikuchi, *Nucl. Fusion* **30**, 265 (1990).

⁸ R. J. Hawryluk, V. Arunasalam, M. G. Bell, M. Bitter, W. R. Blanchard, N. L. Bretz, R. Budny, C. E. Bush, J. D. Callen, S. A. Cohen, S. K. Combs, S. L. Davis, D. L. Dimock, H. F. Dylla, P. C. Efthimion, L. C. Emerson, A. C. England, H. P. Eubank, R. J. Fonck, E. D. Fredrickson, H. P. Furth, G. Gammel, R. J. Goldston, B. Grek, L. R. Grisham, G. W. Hammett, W. W. Heidbrink, H. W. Hendel, K. W. Hill, E. Hinnov, S. Hiroe, H. Hsuan, R. A. Hulse, K. P. Jaehnig, D. L. Jassby, F. C. Jobs, D. W. Johnson, L. C. Johnson, R. Kaita, R. Kamperschroer, S. M. Kaye, S. J. Kilpatrick, R. J. Knize, H. Kugel, P. H. LaMarche, B. LeBlanc, R. Little, C. H. Ma, D. M. Manos, D. K. Mansfield, R. T. McCann, M. P. McCarthy, D. C. McCune, K. McGuire, D. H. McNeill, D. M. Meade, S. S. Medley, D. R. Mikkelsen, S. L. Milora, W. Morris, D. Mueller, V. Mukhovatov, E. B. Nieschmidt, J. O'Rourke, D. K. Owens, H. K. Park, N. Pomphrey, B. Prichard, A. T. Ramsey, M. H. Redi, A. L. Roquemore, P. H. Rutherford, N. R. Sauthoff, G. Schilling, J. Schivell, G. L. Schmidt, S. D. Scott, S. Sesnic, J. C. Sillis, F. J. Stauffer, B. C. Stratton, G. D. Tait, G. Taylor, J. R. Timberlake, H. H. Towner, M. Ulrickson, V. Vershkov, S. Von Goeler, F. Wagner, R. Wieland, J. B. Wilgen, M. Williams, K.-L. Wong, S. Yoshikawa, R. Yoshino, K. M. Young, M. C. Zarnstorff, V. S. Zaveryaev,

- and S. J. Zweben, in *Plasma Physics and Controlled Nuclear Fusion Research*, Proceedings of the 11th International Conference, Kyoto, 1986 (IAEA, Vienna, 1987), Vol. 1, p. 51.
- ⁹ A. V. Deniz, X. L. Li, and T. C. Marshall, *Phys. Fluids* **30**, 2527 (1987).
- ¹⁰ T. C. Simonen, M. Matsuoka, D. K. Bhadra, K. H. Burrell, R. W. Callis, M. S. Chance, M. S. Chu, J. M. Greene, R. J. Groebner, R. W. Harvey, D. N. Hill, J. Kim, L. Lao, P. I. Petersen, G. D. Porter, H. St. John, B. W. Stallard, R. D. Stambaugh, E. J. Strait, and T. S. Taylor, *Phys. Rev. Lett.* **61**, 1720 (1988).
- ¹¹ A. W. Morris, R. Fitzpatrick, P. S. Haynes, T. C. Hender, J. Hugill, C. Silvester, and T. N. Todd, in *Proceedings of the 17th European Conference on Controlled Fusion and Plasma Heating*, Amsterdam (EPS, Petit-Lancy, Switzerland, 1990), Vol. 14B, Part I, p. 379.
- ¹² S. C. Luckhardt, K.-I. Chen, S. Coda, J. Kesner, R. Kirkwood, B. Lane, M. Porkolab, and J. Squire, *Phys. Rev. Lett.* **62**, 1508 (1989).
- ¹³ J. D. Strachan, M. Bitter, A. T. Ramsey, M. C. Zarnstorff, V. Arunasalam, M. G. Bell, N. L. Bretz, R. V. Budny, C. E. Bush, D. L. Davis, H. F. Dylla, P. C. Efthimion, R. J. Fonck, E. D. Fredrickson, H. P. Furth, R. J. Goldston, B. Grek, L. R. Grisham, R. J. Hawryluk, W. W. Heidbrink, H. W. Hendel, K. W. Hill, H. Hsuan, K. P. Jaehnig, D. L. Jassby, F. C. Jobs, D. W. Johnson, L. C. Johnson, R. Kaita, J. Kamperschroer, R. J. Knize, T. Kozub, H. Kugel, B. LeBlanc, F. Levinton, P. H. LaMarche, D. M. Manos, D. K. Mansfield, K. M. McGuire, D. H. McNeill, D. M. Meade, S. S. Medley, W. Morris, D. Mueller, E. B. Nieschmidt, D. K. Owens, H. K. Park, J. Schivell, G. Schilling, G. L. Schmidt, S. D. Scott, S. Sesnic, J. C. Sennis, F. J. Stauffer, B. C. Stratton, G. D. Tait, G. Taylor, H. H. Towner, M. Ulrickson, S. Von Goeler, R. Wieland, M. D. Williams, K.-L. Wong, S. Yoshikawa, K. M. Young, and S. J. Zweben, *Phys. Rev. Lett.* **58**, 1004 (1987).
- ¹⁴ K. McGuire, V. Arunasalam, C. W. Barnes, M. G. Bell, M. Bitter, H.-S. Bosch, N. L. Bretz, R. Budny, C. E. Bush, A. Cavallo, P. L. Colestock, S. L. Davis, D. L. Dimock, H. F. Dylla, P. C. Efthimion, A. B. Ehrhardt, R. J. Fonck, E. D. Fredrickson, R. J. Goldston, G. J. Greene, B. Grek, L. R. Grisham, G. W. Hammet, R. J. Hawryluk, H. W. Hendel, K. W. Hill, E. Hinnov, R. B. Howell, H. Hsuan, K. P. Jaehnig, D. L. Jassby, F. C. Jobs, D. W. Johnson, L. C. Johnson, R. Kaita, S. J. Kilpatrick, R. J. Knize, G. Kuo-Petravic, P. H. LaMarche, D. M. Manos, J. Manickam, D. K. Mansfield, R. T. McCann, M. P. McCarthy, D. C. McCune, D. H. McNeill, D. M. Meade, S. S. Medley, D. R. Mikkelsen, A. Miller, W. Morris, D. Mueller, E. B. Nieschmidt, D. K. Owens, H. K. Park, N. Pomphrey, A. T. Ramsey, M. H. Redi, P. H. Roquemore, T. Saito, N. R. Sauthoff, G. Schilling, J. Schivell, G. L. Schmidt, S. D. Scott, J. C. Sennis, J. E. Stevens, W. Stodiek, B. C. Stratton, G. D. Tait, G. Taylor, J. R. Timberlake, H. H. Towner, M. Ulrickson, S. Von Goeler, R. Wieland, M. Williams, K.-L. Wong, S. Yoshikawa, K. M. Young, M. C. Zarnstorff, and S. J. Zweben, *Plasma Phys. Controlled Fusion* **30**, 1391 (1988).
- ¹⁵ F. Troyon, R. Gruber, H. Saurenmann, S. Semenzato, and S. Succi, *Plasma Phys. Controlled Fusion* **26** 1A, 209 (1984); *Phys. Lett.* **110A**, 29 (1985).
- ¹⁶ M. G. Bell, V. Arunasalam, C. W. Barnes, M. Bitter, H.-S. Bosch, N. L. Bretz, R. Budny, C. E. Bush, A. Cavallo, T. K. Chu, S. A. Cohen, P. L. Colestock, S. L. Davis, D. L. Dimock, H. F. Dylla, P. C. Efthimion, A. B. Ehrhardt, R. J. Fonck, E. D. Fredrickson, H. P. Furth, G. Gammel, R. J. Goldston, G. J. Greene, B. Grek, L. R. Grisham, G. W. Hammet, R. J. Hawryluk, H. W. Hendel, K. W. Hill, E. Hinnov, J. C. Hosea, R. B. Howell, H. Hsuan, R. A. Hulse, K. P. Jaehnig, A. C. Janos, D. L. Jassby, F. C. Jobs, D. W. Johnson, L. C. Johnson, R. Kaita, C. Kieras-Phillips, S. J. Kilpatrick, V. A. Krupin, P. H. LaMarche, W. D. Langer, B. LeBlanc, R. Little, A. I. Lysojvan, D. M. Manos, D. K. Mansfield, E. Mazzucato, R. T. McCann, M. P. McCarthy, D. C. McCune, K. M. McGuire, D. H. McNeill, D. M. Meade, S. S. Medley, D. R. Mikkelsen, R. W. Motley, D. Mueller, Y. Murakami, J. A. Murphy, E. B. Nieschmidt, D. K. Owens, H. K. Park, A. T. Ramsey, M. H. Redi, A. L. Roquemore, P. H. Rutherford, T. Saito, N. R. Sauthoff, G. Schilling, J. Schivell, G. L. Schmidt, S. D. Scott, J. C. Sennis, J. E. Stevens, W. Stodiek, B. C. Stratton, G. D. Tait, G. Taylor, J. R. Timberlake, H. H. Towner, M. Ulrickson, S. Von Goeler, S. Yoshikawa, K. M. Young, M. C. Zarnstorff, and S. J. Zweben, in *Plasma Physics and Controlled Nuclear Fusion Research*, Proceedings of the 12th International Conference, Nice, 1988 (IAEA, Vienna, 1989), Vol. 1, p. 27.
- ¹⁷ R. J. Goldston, D. C. McCune, H. H. Towner, S. L. Davis, R. J. Hawryluk, and G. L. Schmidt, *J. Comput. Phys.* **43**, 61 (1981).
- ¹⁸ D. W. Swain and G. H. Neilson, *Nucl. Fusion* **22**, 1015 (1982).
- ¹⁹ L. L. Lao, H. St. John, R. D. Stambaugh, and W. Pfeiffer, *Nucl. Fusion* **25**, 1421 (1985).
- ²⁰ M. E. Mauer, T. H. Ivers, H. Y. Che, D. Chen, D. Gates, T. C. Marshall, G. A. Navratil, J. Wang, D. S. Darrow, M. Ono, in Ref. 16, p. 415.
- ²¹ L. L. Lao, H. St. John, R. D. Stambaugh, A. G. Kellman, W. Pfeiffer, *Nucl. Fusion* **25**, 1611 (1985).
- ²² E. S. Marmor, J. L. Terry, B. Lipshultz, and J. E. Rice, *Rev. Sci. Instrum.* **60**, 3739 (1989).
- ²³ C. E. Bush, R. J. Goldston, S. D. Scott, E. D. Fredrickson, K. McGuire, J. Schivell, G. Taylor, C. W. Barnes, M. G. Bell, R. L. Boivin, N. Bretz, R. V. Budny, A. Cavallo, P. C. Efthimion, B. Grek, R. Hawryluk, K. Hill, R. A. Hulse, A. Janos, D. W. Johnson, S. Kilpatrick, D. M. Manos, D. K. Mansfield, D. M. Meade, H. Park, A. T. Ramsey, B. Stratton, E. J. Synakowski, H. H. Towner, R. M. Wieland, M. C. Zarnstorff, and S. J. Zweben, *Phys. Rev. Lett.* **65**, 424 (1990).
- ²⁴ K. Toi, K. Kawahata, S. Morita, T. Watari, R. Kumazawa, K. Ida, A. Ando, Y. Oka, M. Sakamoto, Y. Hamada, K. Adati, R. Ando, T. Aoki, S. Hidekuma, S. Hirokura, O. Kaneko, A. Karita, T. Kawamoto, Y. Kawasumi, T. Kuroda, K. Masai, K. Narihara, Y. Ogawa, K. Ohkubo, S. Okajima, T. Ozaki, M. Sasao, K. N. Sato, T. Seki, F. Shimpou, H. Takahashi, S. Tanahashi, Y. Taniguchi, and T. Tsuzuki, *Phys. Rev. Lett.* **64**, 1895 (1990).
- ²⁵ E. J. Strait, J. R. Ferron, L. L. Lao, T. S. Taylor, M. S. Chu, F. J. Helton, W. L. Howl, A. G. Kellman, E. Lazarus, J. K. Lee, T. H. Osborne, R. D. Stambaugh, and A. D. Turnbull, *Bull. Am. Phys. Soc.* **34**, 1939 (1989).
- ²⁶ P. N. Yushmanov, T. Takizuka, K. S. Riedel, O. J. W. F. Kardaun, J. G. Cordey, S. M. Kaye, D. E. Post, *Nucl. Fusion* **30**, 1999 (1990).
- ²⁷ M. C. Zarnstorff, B. Grek, D. W. Johnson, D. K. Mansfield, E. S. Marmor, H. K. Park, A. T. Ramsey, J. Schivell, S. D. Scott, B. C. Stratton, E. J. Synakowski, G. Taylor, and J. L. Terry, *Bull. Am. Phys. Soc.* **35**, 2108 (1990).
- ²⁸ H. Murmann, H. Zohm, and the ASDEX- and NI team, in *Proceedings of the 17th European Conference on Controlled Fusion and Plasma Heating*, Amsterdam (EPS, Petit-Lancy, Switzerland, 1990), Vol. 14B, Part I, p. 54.
- ²⁹ D. L. Jassby and the TFTR Group, *Bull. Am. Phys. Soc.* **35**, 1917 (1990); *Phys. Fluids B* **3**, 2308 (1991).